Transmission and reflection of transverse-magnetic-polarized optical fields at stratified nonlinear media

U. Trutschel, F. Lederer, and U. Langbein
Sektion Physik, Friedrich-Schiller-Universität Jena, DDR-6900 Jena, German Democratic Republic
(Received 10 April 1989)

For the first time we study the transmission and the reflection of transverse-magnetic-polarized optical fields which impinge obliquely on diverse multilayer systems showing distinct resonances of geometrical origin in the low-intensity limit. The individual layers are endowed with nonlinear materials, the complex dielectric functions of which depend on the local intensity of the optical wave. The field propagation is described by a straightforward algorithm that reduces the final field calculation to a standard Runge-Kutta procedure. With respect to varying input fluxes we discuss in detail the response characteristic of a single nonlinear film near the angle of total internal reflection, a nonlinear periodic multilayer system near the edges of its stop gap, and a nonlinear Fabry-Pérot Étalon, coated with linear or nonlinear dielectric mirrors, near an Airy resonance, respectively. For all configurations under investigation, a bistable input-output flux characteristic is predicted. We compare also the response behavior as it depends on the state of polarization. A clear advantage of transverse electric polarized fields with respect to lower switching intensities could be identified. There are indications for optical bistability with respect to the polarization angle.

I. INTRODUCTION

In recent years, there has been a rapidly increasing interest in the theoretical and experimental study of the propagation of electromagnetic radiation in materials whose dielectric tensor varies with the amplitude or intensity of the optical field. When such materials are implemented in thin optical films or stratified media, the field propagation is altered by the presence of interfaces, which leads to exciting properties of the pertinent optical response characteristic, such as power-flux-controlled detuning of transmission resonances accompanied by optical-bistability- and -multistability phenomena. These phenomena result from an interplay of refraction, reflection and phase-matched interference effects of optically linear and/or nonlinear origin, and have a great potential to all-optical information processing applications.[1]

The scope of the present paper is the full electromagnetic description of the optical response behavior of nonlinear stratified media under plane-wave irradiation, with conditions where perturbation theories do not apply. To keep this paper within reasonable limits, we will exclude the consideration of guided wave fields, although requiring similar mathematical techniques. Preliminary results on this topic can be found elsewhere.[2]

The pertinent theoretical analysis splits into two fundamental parts, namely the integration of the nonlinear wave equation with suitable boundary conditions and the proper consideration of the electromagnetic crossing conditions along each interface. The complexity of both parts is essentially determined by the assumed polarization of the total optical field as well as the choice of the relevant dielectric tensors.

Transverse-electric (TE) -polarized fields are characterized by a single electric field component pointing perpendicular to the plane of incidence. Hence, the whole problem reduces to a scalar one.

For transverse-magnetic (TM) -polarized fields, the occurrence of two field components, one pointing parallel and one perpendicular to the interfaces, leads, in general, to a nondiagonal nonlinear dielectric tensor even for materials that are isotropic in the low-intensity limit. This circumstance complicates both parts of the analysis appreciably.

To our best knowledge, the theoretical program outlined so far has been performed for TE-polarized optical fields only propagating in various nonlinear thin-film geometries.[3–9] These studies cover normal and oblique[4,5,9] plane-wave incidence, and nonlinear refractive-index saturation[4,9] and absorption.[9]

All these studies found the incident power flow as an essential tuning parameter. When exceeding certain power-flow thresholds, the optical response characteristic becomes multivalued and optical bistability sets in.

The formation of multivalued response curve sections can be understood as a field-induced detuning of sharp transmission resonance peaks already occurring in the low-intensity limit, i.e., under optically linear conditions. (These resonances will be labeled "linear resonances" determined by the linear optical properties of the system.) With increasing power flow, the material nonlinearities provoke a shift of the total resonance peak accompanied by a steepening of one peak slope until the whole peak inclines so extremely that the peak slope gets bent back.

These effects have been predicted, respectively, for single nonlinear films illuminated under total-internal-reflection (TIR) conditions[4,5] or by introducing large refractive-index differences between the film and its environment,[3,5] and for nonlinear periodic multilayer systems illuminated near the appropriate edge of the stop gap determined by linear lattice theory. In this case, the emerging field profiles, associated with a transmission reso-

nance that is pushed into the stop-gap region, have been identified as so-called "gap solitons".[6–8]

Eventually, two classical studies closely related to our topic, shall be mentioned. Marburger and Felber[10] considered for the first time the optical response of a nonlinear layer but with boundary conditions which suppose the layer is bounded by perfect mirrors. Winful, Marburger, and Garmire[11] predicted first optical bistability in nonlinear distributed-feedback structures. We mention also the consideration of a Fabry-Pérot cavity, composed of a nonlinear film, both endfaces of which are provided with optically linear highly reflecting multilayer coatings, in the framework of a slowly varying envelope approximation.[12]

The program of the present paper is twofold in the sense that both a theoretical analysis of the nonliner response problem for TM-polarized optical fields shall be provided, complemented by the detailed investigation of several well-designed composite thin-film geometries.

The theoretical analysis leads to a straightforward but very flexible algorithm that describes the steady-state response behavior of a mixed-type linear and/or nonlinear multilayer system for a TM-polarized obliquely incident plane wave. This algorithm is well adapted to multilayer problems and permits the inclusion of both linear and nonlinear absorption as well as saturation of the nonlinearity and reduces the final numerical-field calculation to a standard Runge-Kutta procedure (Secs. II and III).

In the numerical part (Sec. IV) we apply the algorithm to several nonlinear film configurations properly designed to show sharp linear transmission resonances. We start with a single, uncoated nonlinear film as the elementary unit of all composite geometries. In our specific example, the input field impinges in the vicinity of the total-internal-reflection angle. Our results complement analogous considerations for TE-polarized fields.[4,5]

Secondly, we consider a periodic multilayer system of 50 unit cells where each unit cell consists of a linear-nonlinear double layer. Here we focus our attention to the edges of a specific stop band of the angular response curve. We find optical bistability and compare our results with analogous studies for the TE case.[6,7,9]

Eventually, we combine both configurations assuming a central nonlinear film (Fabry-Pérot cavity) both endfaces of which are coated by either a linear or a nonlinear periodic multilayer system. The interplay of both configurations gives rise to sharp Airy resonance peaks in the gap region of the multilayer cladding. These resonances are very sensitive to nonlinear detuning leading to bistable response curves. A comparison, both with TE-polarized incident fields and with two uniaxial approximations, frequently used for TM-polarized fields, concludes the numerical part of this paper.

In order to keep the number of tunable parameters within reasonable limits, we restrict our numerical studies (Sec. IV) to dispersive, nonsaturating Kerr-type nonlinearities, leaving the inclusion of more subtle nonlinearities to a forthcoming paper. However, the effect of *linear* absorption has been considered. For TE-polarized fields, the influence of nonlinear absorption and saturation effects on the response behavior of a periodic multilayer system has been studied recently.[9]

As far as we can see, the present study gives the first survey on the TM-optical response of nonlinear stratified media based on an exact integration of the nonlinear field equations, even under the simplifying assumptions summarized above.

II. THE OPTICAL FIELD IN A NONLINEAR MULTILAYER SYSTEM

We consider a multilayer system where the interfaces are parallel to the x coordinate and the plane of incidence shall coincide with the x-z plane. Hence, the geometry shows a translational invariance with respect to the y coordinate.

We assume TM polarization and investigate the steady-state response of the system under oblique plane-wave incidence.

Hence, the electric (E_x, E_z) and magnetic field $(B_y = B)$ components (symbolically denoted by A) are of the form

$$A(X,Z,t) = A(Z)\exp[i(\beta X - \omega t)] + \text{c.c.}\ , \tag{1}$$

where $X = kx$ and $Z = kz$ are scaled parameters, with $k = \omega/c$, and β is the normalized x component of the wave vector.

We are only interested in automatically phase-matched third-order off-resonant nonlinear processes. Hence, we can restrict the analysis to that part of the nonlinear polarization oscillating with the frequency ω. Under these conditions, the nonlinear polarization in a linearly isotropic crystal can be written as[12,13]

$$P_i^{\mathrm{NL}}(x,z) = \epsilon_0 \chi_{ik}^{\mathrm{NL}} E_k \tag{2}$$

with

$$\chi_{ik}^{\mathrm{NL}} = \chi[D(E_i E_k^* + E_i^* E_k) + (C - D)|\mathcal{E}|^2 \delta_{ik}], \quad i,k = x,z$$

where C and D are constants related to the physical origin of the nonlinearity and χ is the constant of the nonlinear interaction. Electronic as well as molecular reorientational-based nonlinearities yield both $C \neq D \neq 0$ leading to nondiagonal tensor χ_{ik}^{NL}.[13] For the sake of clearness we restrict our analysis to the simplest case where the "anisotropy" vanishes $(D = 0)$. This type of nonlinear polarization is produced by electrostriction and thermal effects.[13] With

$$\mathcal{D}(x,z) = \bar{\epsilon}\epsilon_0 \mathcal{E}(x,z) + \mathcal{P}^{\mathrm{NL}}(x,z)$$

we can introduce the nonlinear dielectric subtensor

$$\hat{\epsilon}_{\mathrm{NL}}(|\mathcal{E}|^2) = \begin{bmatrix} \epsilon_{xx}(|\mathcal{E}|^2) & 0 \\ 0 & \epsilon_{zz}(|\mathcal{E}|^2) \end{bmatrix} \tag{3}$$

with

$$\epsilon_{ii} = \bar{\epsilon} + \alpha(|E_x|^2 + |E_z|^2), \quad i = x,z \tag{4a}$$

where $\alpha = \chi C$ is the nonlinear and $\bar{\epsilon} = \bar{\epsilon}' + i\bar{\epsilon}''$ the complex linear dielectric coefficient. In our general analysis we make no access to the explicit form of the tensor ele-

ments ϵ_{xx} and ϵ_{zz} thus permitting the phenomenological inclusion of saturation as well as nonlinear absorption effects. Both effects can be phenomenologically taken into account in writing the tensor elements as

$$\epsilon_{ii}=\bar{\epsilon}+\alpha C_{ii}^2\left[1-\exp\left[\frac{|E_x|^2+|E_z|^2}{C_{ii}^2}\right]\right],\quad i=x,z \tag{4b}$$

where C_{xx}, C_{zz} are constants and α is now a complex-valued quantity. The maximum field-induced dielectric coefficients are then

$$\epsilon_{ii}=\bar{\epsilon}+\alpha C_{ii}^2 ,$$

and the dispersive Kerr nonlinearity is reestablished in the low-intensity limit and setting $\alpha=\alpha^*$. This is only one way to model saturation and nonlinear absorption effects but shall suffice for the present purpose.

With the ansatz (1) and Eqs. (3) and (4) Maxwell's equations reduce to

$$dE_x/dZ=i(cB+\beta E_z) , \tag{5a}$$

$$dB/dZ=\frac{i}{c}\epsilon_{xx}E_x , \tag{5b}$$

$$E_z=-\frac{\beta_c}{\epsilon_{zz}}B . \tag{5c}$$

Taking advantage of Eq. (5c), the magnetic field B can be replaced in favor of the E_z component of the electric field. This leads to a set of equations which contain the electric fields exclusively,

$$dE_x/dZ=\frac{i}{\beta}(\beta^2-\epsilon_{zz})E_z , \tag{6a}$$

$$d(\epsilon_{zz}E_z)/dZ=-i\beta\epsilon_{xx}E_x . \tag{6b}$$

Recalling that ϵ_{xx} and ϵ_{zz} depend not only on E_x and E_z, but also on the complex conjugate fields, E_x^* and E_z^* must be also at our disposal. In order to get a system of differential equations that can be handled by a standard Runge-Kutta procedure, the differentiation both in Eq. (6b) and its complex conjugate counterpart must be carried out. Additionally, the complex conjugate of Eq. (6a) must be introduced. The differentiation procedure is straightforward, but very tedious, and shall not be detailed here.

Eventually, we end up with our fundamental system of differential equations

$$dE_x/dZ=\frac{i}{\beta}(\beta^2-\epsilon_{zz})E_z , \tag{7a}$$

$$dE_x^*/dZ=-\frac{i}{\beta}(\beta^2-\epsilon_{zz}^*)E_z^* , \tag{7b}$$

$$dE_z/dZ=-\frac{i}{\beta}\frac{\beta^2E_z[\epsilon_{xx}(d\epsilon_{zz}^*/dI)E_xE_z^*+\epsilon_{xx}^*(d\epsilon_{zz}/dI)E_x^*E_z]+\epsilon_{xx}\epsilon_{zz}^*\beta^2E_x}{(d|\epsilon_{zz}|^2/dI)|E_z|^2+|\epsilon_{zz}|^2}$$
$$-\frac{i}{\beta}\frac{\epsilon_{zz}^*E_z(d\epsilon_{zz}/dI)[E_x^*E_z(\beta^2-\epsilon_{zz})-E_xE_z^*(\beta^2-\epsilon_{zz}^*)]}{(d|\epsilon_{zz}|^2/dI)|E_z|^2+|\epsilon_{zz}|^2} , \tag{7c}$$

$$dE_z^*/dZ=\frac{i}{\beta}\frac{\beta^2E_z^*[\epsilon_{xx}(d\epsilon_{zz}^*/dI)E_xE_z^*+\epsilon_{xx}^*(d\epsilon_{zz}/dI)E_x^*E_z]+\epsilon_{xx}^*\epsilon_{zz}\beta^2E_x^*}{(d|\epsilon_{zz}|s/dI)|E_z|^2+|\epsilon_{zz}|^2}$$
$$-\frac{i}{\beta}\frac{\epsilon_{zz}E_z^*(d\epsilon_{zz}^*/dI)[E_x^*E_z(\beta^2-\epsilon_{zz})-E_xE_z^*(\beta^2-\epsilon_{zz}^*)]}{(d|\epsilon_{zz}|^2/dI)|E_z|^2+|\epsilon_{zz}|^2} , \tag{7d}$$

where the explicit dependence of the tensor elements (4a) and (4b) on the local intensity $I=|E_x|^2+|E_z|^2$ was used.

Now, our aim consists of calculating the field components E_x, E_x^*, E_z, and E_z^* at the exit interface of both a single nonlinear layer and a multilayer system assuming that all field components involved are known at the entrance interface. Note that the proper relation among the "initial" field components will be established in Sec. III when the incident and transmitted fields are introduced. Additionally, we must recall the discontinuity of E_z and E_z^* when crossing the entrance interface. Due to the continuity of B, E_x, and E_x^* along the interfaces, we get from Eq. (5c)

$$\epsilon_{zz-}(|E_x|^2,|E_{z-}|^2)E_{z-}=\epsilon_{zz+}(|E_x|^2,|E_{z+}|^2)E_{z+} , \tag{8a}$$

$$\epsilon_{zz-}^*(|E_x|^2,|E_{z-}|^2)E_{z-}^*=\epsilon_{zz+}^*(|E_x|^2,|E_{z+}|^2)E_{z+}^* , \tag{8b}$$

where both the fields and the tensor elements before and beyond the interface are labeled by $-$ or $+$ signs, respectively. Both Eqs. (8) must be solved simultaneously by numerical means in order to get E_{z+} and $(E_{z+})^*$, provided that E_{z-} and $(E_{z-})^*$ are known. Most conveniently, this can be performed by an iteration procedure using the initial values

$$E_{z+}=\frac{\epsilon_{zz-}(|E_x|^2,|E_{z-}|^2)}{\bar{\epsilon}_+}E_{z-} ,$$
$$E_{z+}^*=\frac{\epsilon_{zz-}^*(|E_x|^2,|E_{z-}|^2)}{\bar{\epsilon}_+^*}E_{z-}^* . \tag{9}$$

Now, all information needed to solve the system (7) by a standard Runge-Kutta procedure is available. We integrate the set of differential equations through the first nonlinear film. At the interface to the second film, characterized by different parameters ϵ and α, the procedure (8) must be repeated. Thus one gets the initial values for the next integration. Eventually, one ends up with the fields E_x, E_x^*, E_z, and E_z^* at the exit interface of the nonlinear multilayer system.

Very recently, Joseph and Christodoulides[14] have found a first integral of the set of equations (6) for guided fields ($E_x, E_z, B \to 0$ for $z \to \infty$) and vanishing losses. With the help of this first integral they succeeded in calculating the fields by a simple quadrature. In our case this approach fails to work because, in contrast to the guided wave scheme, the fields within the films are no longer real-valued and we allow for linear losses.

III. THE OPTICAL RESPONSE OF THE NONLINEAR MULTILAYER SYSTEM

We assume the following geometry. A linear substrate (ϵ_s) shall occupy the half-space $z<0$. This substrate is loaded by a stack of nonlinear films forming N unit cells. Each unit cell shall be composed of two different films characterized by the complex dielectric tensors $\hat{\epsilon}_{\mathrm{NL}a}, \hat{\epsilon}_{\mathrm{NL}b}$ and the thicknesses $d_{\mathrm{NL}a}, d_{\mathrm{NL}b}$, respectively. The overall thickness of the stack is $D_{\mathrm{ML}}=N(d_{\mathrm{NL}a}+d_{\mathrm{NL}b})$. Eventually the stratified medium is covered by a linear cladding (ϵ_c) occupying the half-space $z \geq D_{\mathrm{ML}}$.

In order to calculate the transmittance and the reflectivity of the system under investigation we must relate the involved fields at the entrance and the exit interface of the nonlinear stack to the substrate and the cladding fields via the boundary conditions. To this end the fields within both the cladding and the substrate have to be detailed.

For both half-spaces the tensor components of ϵ_{NL} simplify to $\epsilon_{xx}=\epsilon_{zz}=\epsilon$, where ϵ stands for ϵ_c and ϵ_s. Note that all quantities applying to the cladding and the substrate are labeled by the subscripts c and s, respectively. Hence the system (6) can be rewritten as PM

$$d^2E_x(Z)/dZ^2+k_z^2E_x(Z)=0 , \tag{10a}$$

$$E_z(Z)=i\frac{\beta}{k_z^2}dE_x(Z)/dZ \tag{10b}$$

with $k_z=(\epsilon-\beta^2)^{1/2}$. Without loss of generality we assume that the dielectric coefficients of the substrate ($\epsilon=\epsilon_s$) and the cladding ($\epsilon=\epsilon_c$) are real valued. Assuming a plane incident wave in the cladding, the total cladding field represents a superposition of the incident and the reflected wave. The corresponding solutions to Eqs. (10) are

$$E_{xc}(Z)=E_x^{\mathrm{in}}\exp[-ik_{zc}(Z-\bar{Z})] + E_x^r\exp[ik_{zc}(Z-\bar{Z})] , \tag{11a}$$

$$E_{zc}(Z)=\frac{\beta}{k_{cz}}\{E_{xc}^{\mathrm{in}}\exp[ik_{zc}(Z-\bar{Z})] - E_{xc}^r\exp[ik_{zc}(Z-\bar{Z})]\} \tag{11b}$$

with $\bar{Z}=kD_{\mathrm{ML}}$. The substrate field is the transmitted field

$$E_{xs}(Z)=E_x^t\exp(ik_{zs}Z) , \tag{12a}$$

$$E_{zs}(Z)=-\frac{\beta}{k_{zs}}E_x^t\exp(-ik_{zs}Z) , \tag{12b}$$

where the superscripts in, r, and t label the incident, reflected, and transmitted fields, respectively. For $Z=0$ Eq. (12a) implies

$$E_{xs}(0)=E_x^t , \tag{13}$$

and from Eqs. (11) one gets at $Z=\bar{Z}$

$$E_{xc}(\bar{Z})=E_x^{\mathrm{in}}+E_x^r, \quad \frac{k_{zc}}{\beta}E_{zc}(\bar{Z})=E_x^{\mathrm{in}}-E_x^r .$$

Taking advantage of the continuity of E_x and $\epsilon_{zz}E_z$, together with the corresponding complex-conjugate quantities, we can replace the cladding fields at the cladding-multilayer system interface by the corresponding interface fields within the nonlinear region. In doing so, we end up with

$$E_x^{\mathrm{in}}=\frac{1}{2}\left[E_x(\bar{Z})+\frac{k_{zc}\epsilon_{zz}(\bar{Z})}{\beta\epsilon_c}E_z(\bar{Z})\right] , \tag{14a}$$

$$E_x^r=\frac{1}{2}\left[E_x(\bar{Z})-\frac{k_{zc}\epsilon_{zz}(\bar{Z})}{\beta\epsilon_c}E_z(\bar{Z})\right] . \tag{14b}$$

Equations (13) and (14) express the desired relations between the field amplitudes at the outermost stack interfaces and the incident and exit fields. Note that there only two parameters free of choice remaining, say E_x^t and E_x^{t*}. Once both (and β) have been fixed, all other parameters are determined by the algorithm.

The final goal consists of calculating the response of the system as it depends on the angle of incidence as well as the input flux. The transmittance and the reflectivity are, respectively, given by

$$T=\frac{S_z^t}{S_z^{\mathrm{in}}} , \tag{15a}$$

$$R=\frac{S_z^r}{S_z^{\mathrm{in}}} , \tag{15b}$$

where S_z is the z component of the time-averaged Poynting vector

$$S_z=\tfrac{1}{2}\mathrm{Re}(E\times H^*)n_z = \frac{\epsilon}{2\mu_0 ck_z}|E_x|^2 . \tag{16}$$

Using Eqs. (13) and (14) one arrives at

$$T=4\frac{k_{zc}\epsilon_s|E_x^t|^2}{k_{zs}\epsilon_c\left|E_x(\bar{Z})+\frac{k_{zc}\epsilon_{zz}(\bar{Z})}{\beta\epsilon_c}E_z(\bar{Z})\right|^2}, \tag{17}$$

$$R=\frac{\left|E_x(\bar{Z})-\frac{k_{zc}\epsilon_{zz}(\bar{Z})}{\beta\epsilon_c}E_z(\bar{Z})\right|^2}{\left|E_x(\bar{Z})+\frac{k_{zc}\epsilon_{zz}(\bar{Z})}{\beta\epsilon_c}E_z(\bar{Z})\right|^2}. \tag{18}$$

In order to discuss the nonlinear response behavior, these quantities have to be evaluated as they depend on the input flux

$$S_z=\frac{\epsilon_c}{8\mu_0 c k_{zc}}\left|E_x(\bar{Z})+\frac{k_{zc}\epsilon_{zz}(\bar{Z})}{\beta\epsilon_c}E_z(\bar{Z})\right|^2. \tag{19}$$

Now with Eqs. (17)–(19) all necessary information is available to evaluate the nonlinear response of a rather general class of multilayer systems for an obliquely incident p-polarized plane-wave field.

The entire numerical algorithm works as follows.

(1) Fix the incident angle θ to get $\beta=(\epsilon_c)^{1/2}\sin\theta$.

(2) Fix $E_{xs}(0)=E_x^t$. Since the substrate is assumed to be lossless, the phase of E_x^t can be set to zero without loss of generality. This implies $E_{xs}^*(0)=E_{xs}(0)$.

(3) Calculate E_z^t and E_z^{t*} via Eq. (10b) to be

$$E_z^t=E_z^{t*}=\frac{\beta}{k_{zs}}E_x^t .$$

(4) Find the initial values $E_{z+}(0), E_{z+}^*(0)$ needed for the numerical procedure via Eq. (8),

$$\epsilon_s E_z^t=\epsilon_{zz+}(|E_x^t|^2,|E_{z+}(0)|^2)E_{z+}(0) ,$$

$$\epsilon_s E_z^{t*}=\epsilon_{zz+}^*(|E_x^t|^2,|E_{z+}(0)|^2)E_{z+}^*(0) .$$

(5) Integrate the system (7) through the nonlinear stack, bearing in mind the discontinuity of E_z and E_z^*, to get $E_x(\bar{Z})$, $E_x^*(\bar{Z})$, $E_z(\bar{Z})$, $E_z^*(\bar{Z})$. Once all fields at the exit interface $Z=Z^-$ of the stack have been found, both the reflectivity and the transmittance of the nonlinear multilayer system follow directly from Eqs. (16)–(18).

We recall that the algorithm outlined so far is applicable to the whole class of nonlinear saturating and absorbing stratified media which can be described by a dielectric tensor (3) the complex-valued elements of which depend on the local-field intensity $|\mathcal{E}|^2$ via (4a) and (4b).

IV. NUMERICAL RESULTS

For our numerical calculations we use the dielectric tensor elements (4a) with real-valued nonlinear coefficients α. Physically, these tensor components describe an isotropic Kerr-like medium with intensity-dependent dielectric coefficients and linear losses. Furthermore, we compare our results with two uniaxial approximations, frequently used in the literature, namely

$$\epsilon_{xx}=\bar{\epsilon}+\alpha(|E_x|^2),\quad \epsilon_{zz}=\bar{\epsilon} \tag{20}$$

denoted by U_x, and

$$\epsilon_{zz}=\bar{\epsilon}+\alpha(|E_z|^2),\quad \epsilon_{xx}=\bar{\epsilon} \tag{21}$$

denoted by U_z. Note that ϵ is a complex-valued quantity.

Now, we are applying our algorithm to three different stratified configurations. Firstly, we study the TIR phenomenon at a single nonlinear film, secondly, a periodic multilayer system illuminated near the edges of its stop band is considered, and thirdly, the Airy resonances of a nonlinear Fabry-Pérot cavity, endowed with multilayer dielectric mirrors, will be investigated. Furthermore, we compare our results with those that hold for TE polarization. To this end we take advantage of two recently published theoretical models.[4,9]

A. Single nonlinear film near the TIR angle

First, we consider a single, uncoated nonlinear film, illuminated in the vicinity of the TIR angle with both TE- and TM-polarized light. The film medium shall be characterized by dielectric coefficients of the type of (4a), (20), and (21), respectively, in the TM case and by

$$\epsilon_{yy}=\bar{\epsilon}+\alpha|E_y|^2 \tag{22}$$

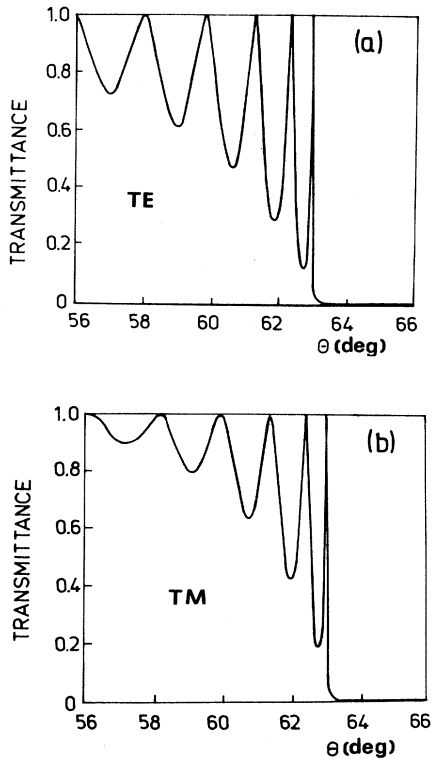

FIG. 1. (a) The transmittance of a single *linear* dielectric film in dependence on the angle of incidence θ near the angle $\theta_{\rm TIR}$ of total internal reflection, for *TE-polarized* fields. The film ($\epsilon_a=2.46$, $d_a=2.5$ μm, $d_b=0$, $N=1$) is embedded between two high index materials ($\epsilon_c=\epsilon_s=3.087$). Other parameters: wavelength $\lambda=2\pi c/\omega=488$ nm (throughout Figs. 1–9), $\theta_{\rm TIR}=63.21°$, $\theta_{\rm res1}=62.99°$ (resonance angle nearest to TIR). (b) The transmittance of the same single *linear* dielectric film as in (a) as a function of the angle of incidence θ for TM-*polarized* fields; same parameters as in (a).

in the TE case, where $\alpha > 0$ is always assumed. The dielectric coefficients $\epsilon_s = \epsilon_c$ of the film surroundings are assumed larger than the linear dielectric coefficient ϵ_a of the film. For there is only a single film unit cell, $N = 1$ and $d_b = 0$ holds, see the initial part of Sec. III for the underlying notation.

The linear angular response curves for TE- as well as TM-polarized fields near the TIR angle θ_{TIR} are plotted in Figs. 1(a) and 1(b), respectively. Due to the larger effective cavity finesse near the TIR angle, the resulting Airy resonances become very sharp thus representing promising candidates for optical bistability. In order to get bistable response curves the input power flow S_z^{in} has been tuned for an incident angle fixed between θ_{TIR} and θ_{rest}, the latter one designating the angular position of the resonance peak nearest to total internal reflection [see Figs. 1(a) and 1(b)]. Note that, for a self-focusing nonlinearity, multivalued sections of the response curve will emerge only at the high-angle slope of the appropriate resonance peak. The nonlinear enhancement of the dielectric coefficients in the nonlinear film shifts both the TIR angle and the peak position slightly towards larger angles. Simultaneously, the peak inclines to the right (i.e., to higher angles) thus leading to the desired backbending of the high-angle peak slope. For defocusing nonlinearities the opposite peak slopes become sensitive to backbending.

The nonlinear response curves are depicted in Fig. 2. Note that any absorption effects have been neglected in this case. As in the TE case,[4] the system shows a distinct bistable behavior.

It is worth pointing out that, within the numerical accuracy, the uniaxial approximation U_z gives the same results as the exact calculations while the U_x approximation fails completely. It is obvious that bistability occurs for the TE case for appreciably smaller input fluxes. Note, on the other hand, that the large transmittance differences between both states of polarization in some input flux intervals indicate the potential occurrence of optical bistability with respect to the polarization angle. This interesting phenomenon deserves further investigations.

B. Periodic multilayer systems

Periodic multilayer systems have attracted a great deal of interest due to their unique optical properties. They show characteristic stop bands the edges of which are very sensitive to a nonlinear detuning as well known for TE-polarized fields.[5,6] For our model configuration we assume a 50-unit-cell multilayer system. Each unit cell consists of two films labeled by a and b. Only the film b with the lower linear dielectric coefficient $\epsilon_b < \epsilon_a$ shall be endowed with a self-focusing Kerr nonlinearity according to Eqs. (4a) and (20)–(22).

For the sake of orientation, we illustrate the angular transmittance curves near the stop band in the linear limit, see Figs. 3(a) and 3(b). The band edges are much steeper in the TE case than in the TM one which will have serious consequences for the power threshold to get

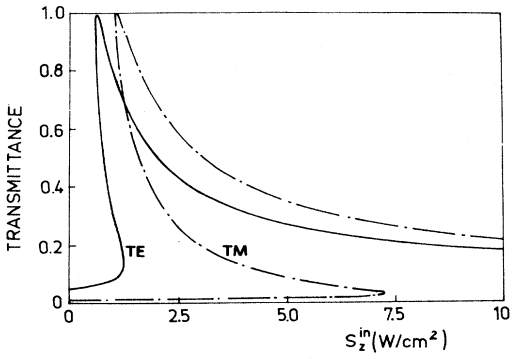

FIG. 2. The transmittance of a single *nonlinear* dielectric film in dependence on the input flux S_z^{in} for a fixed angle of incidence $\theta^{\mathrm{in}} = 63.1°$ and both states of polarization, $\theta_{\mathrm{res1}} < \theta < \theta_{\mathrm{TIR}}$. All linear and geometrical parameters as in Fig. 1(a), $n_{2a} = 2 \times 10^{-9}$ m²/W. (The nonlinear coefficient n_2 is related to α via $\alpha = \epsilon_0 \epsilon c n_2$.) Solid curve, TE-polarization; dashed-dotted curve, TM polarization.

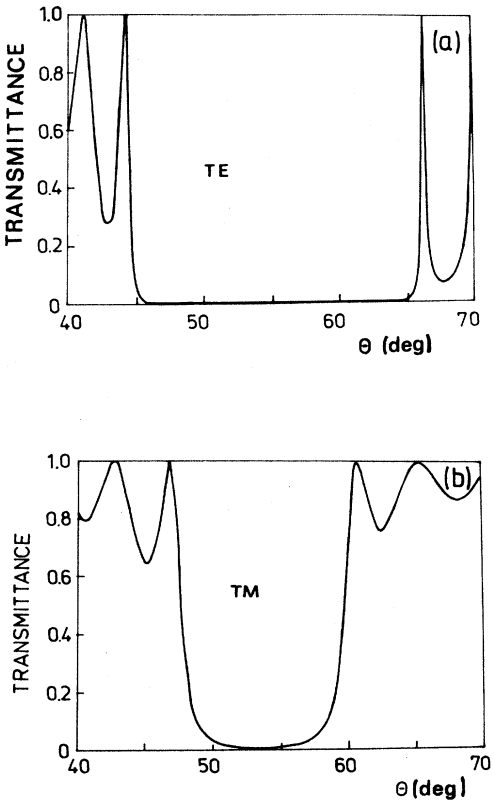

FIG. 3. (a) The stop gap in the angular response curve of a *linear* periodic multilayer system for *TE-polarized* fields: Transmittance vs angle of incidence θ. Parameters: $\epsilon_s = \epsilon_c = 1$, $d_a = 90$ nm, $d_b = 80$ nm, $N = 50$, $\epsilon_a = 2.95$, $\epsilon_b = 2.46$; lower gap edge, $\theta_{\mathrm{TE}}^{\mathrm{le}} = 45.31°$, upper gap edge: $\theta_{\mathrm{TE}}^{\mathrm{ue}} = 64.64°$. (b) Same type of curve as in (a), but for TM-*polarized* fields, all parameters as in (a) except the gap position: Lower gap edge: $\theta_{\mathrm{TM}}^{\mathrm{le}} = 48.71°$, upper gap edge: $\theta_{\mathrm{TM}}^{\mathrm{ue}} = 58.44°$.

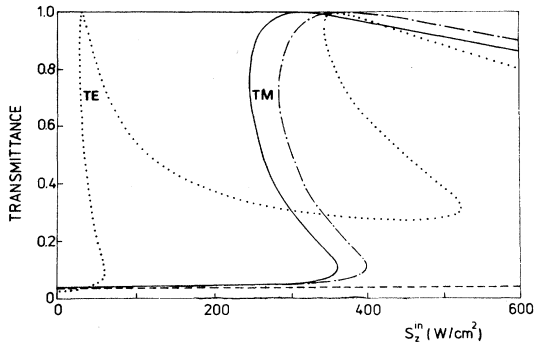

FIG. 4. The response curve of a *nonlinear* periodic multilayer system with a self-focusing nonlinearity ($n_{2b}=2\times10^{-9}$ m²/W) assumed; (Nonlinear counterpart to the linear system underlying Figs. 3). The transmittance is plotted versus the input flux S_z^{in} for fixed angle of incidence θ and both states of polarization as well as for two uniaxial TM approximations (U_x, U_z; see text); all curves apply to the vicinity of the *lower* stop gap edge θ^{le} (see Figs. 3), dotted curve: TE *polarization*, $\theta_{TE}=45.3°$ solid curve: TM*polarization*; dashed-dotted curve: U_x, dashed curve: U_z, $\theta_{TM}=50.0°$, all other parameters as in Figs. 3.

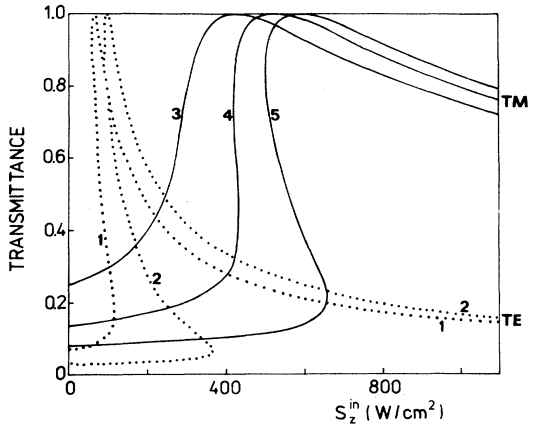

FIG. 6. The evolution of both the TE-polarized (2) and the TM-polarized (5) response curve of Fig. 5 (defocusing nonlinear periodic multilayer system) for different angles of incidence θ near the upper stop gap edge. Dotted curves, TE polarization; solid curves, TM polarization; 1, $\theta_{TE}=65.5°$; 2, $\theta_{TE}=65.2°$; 3, $\theta_{TM}=59.0°$; 4, $\theta_{TM}=58.5°$; 5, $\theta_{TM}=58.0°$. All other parameters as in Fig. 5.

optical bistability.

The onset of the nonlinearity in the nonlinear films increases the average dielectric coefficient of the entire system accompanied by a reduction of the effective "grating modulation." These effects provoke a slight shift of the stop band towards larger incident angles and a shrinkage of the gap width accompanied by a steepening and backbending of the low-angle edge of the stop band. The upper-angle stop band edge gets smoother and hence is of no interest for optical bistability.

In Fig. 4 the transmittance versus incident power curves are depicted for fixed angles of incidence in the proximity of the low-angle band edge. The different power thresholds to get optical bistability for both states of polarization are obvious. The uniaxial approximation U_x provides a rather good agreement with the exact results.

If the sign of the nonlinear coefficient changes (defocusing nonlinear film components) the situation reverses in that now the high-angle band edge becomes sensitive to backbending while the lower-angle edge becomes insensitive. The same phenomenon has been reported by Chen and Mills.[6] Our reasoning follows the same lines given above but with the tendencies reversed. Figure 5 represents the counterpart to Fig. 4 but with incident angles near the upper band edge. Note the reversed validity of both uniaxial approximations.

The increase of the power thresholds to get optical bistability in the defocusing case can be understood also in terms of an effective grating picture where stop band position and width are determined by the effective average dielectric coefficient and the effective grating modulation, respectively. It turns out that, in our configuration, the

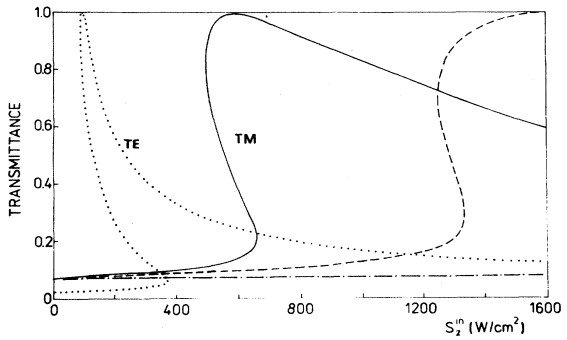

FIG. 5. The response curve of the same nonlinear periodic multilayer system as in Fig. 4, but for incidence angles $\theta_{TE}=65.2°$, $\theta_{TM}=58.0°$ near the *upper* stop gap edge θ^{ue} (see Figs. 3) and self-defocusing nonlinear films ($n_{2b}=-2\times10^{-9}$ m²/W) parameters and curve indication as in Fig. 4. Note the alternating validity of the uniaxial approximations.

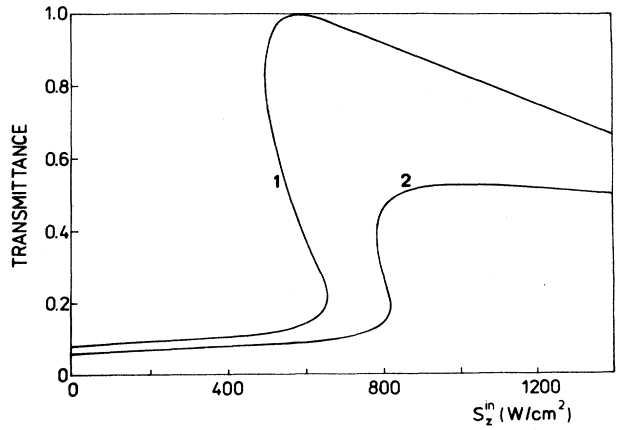

FIG. 7. The modification of the response curve displayed in Fig. 5 (nonlinear periodic multilayer system), due to linear losses, for a fixed angle of incidence $\theta_{TM}=58.0°$ and TM-polarized fields near the upper stop gap edge. Curve 1, without losses (see Fig. 5); curve 2, with losses; $\bar{\epsilon}_b''=0.01$, other parameters as in Fig. 5.

lower band edge is more sensitive to nonlinear changes than the upper one.

A check of the field profiles, related to those parameters where the transmittance approaches unity, revealed the same solitonlike structures as reported by Chen, Mills, and Trullinger[7,8] but now for obliquely incident fields.

In Fig. 6 the effect of different angles of incidence on the shape of the response curves is sketched for both states of polarization near the upper band edge. This system has a differential-gain-like behavior for small detunings and turns to a bistable behavior for larger detunings.

The effect of linear attenuation processes is displayed in Fig. 7. It is evident that the bistable behavior occurs now for larger input fluxes and is less pronounced in comparison with vanishing absorption. Note that the effective absorption length was larger than the entire thickness of the absorbing films. Presumably, the bistable response cannot survive if the situation is reversed.[5,6]

C. Nonlinear Fabry-Pérot etalon with multifilm endface coating

The mechanism responsible for optical bistability in nonlinear Fabry-Pérot etalons is well understood. A self-focusing dispersive nonlinearity provided, the enhancement of the input flux leads to a shift of the Airy resonances towards higher angles of incidence accompanied by a total peak bending with the same tendency.[9,11] Hence, the large-angle slopes of the Airy peaks suffer a backbending intimately connected with optical bistability. In the defocusing case, the opposite slopes become unstable.

For our model configuration we achieve the necessary high endface reflectivity of the cavity film by providing both endfaces with periodic multifilm systems of both linear and nonlinear characteristic driven in the center of an appropriate stop band. This is, in some respect, a combination of both configurations discussed above. Recently, a similar geometry has been studied by Dutta Gupta *et al.*[10] in the framework of a matrix approach that assumes, in contrast to the present study, the slowly varying envelope approximation for the fields within the nonlinear film components. It is evident that we also took advantage of the linear matrix method in calculating the fields in the linear multifilm system components.

The angular transmittance for both states of polarization, in the linear limit, is depicted in Figs.8(a) and 8(b). The Airy-like resonances of the central Fabry-Pérot cavity emerging within the stop bands of the periodic multifilm coating can be clearly identified (compare also Fig. 8 with Fig. 3). Again the TE resonances turn out much sharper than the TM ones. We admit, however, that the similar high reflectivity values of our 25-unit-cell coating can be obtained by a properly designed system of considerably less unit cells, too.

The transmittance versus input flux response curves have been plotted for the angles of incidence according to the large-angle slope of an Airy-like resonance $\theta_{\rm res}$ in the very center of the coating stop band (see Fig.9). It does not surprise us that the use of a *nonlinear* multifilm coat-

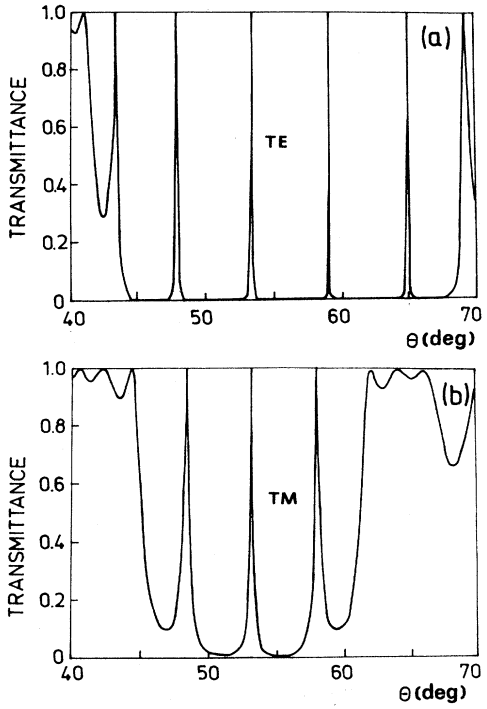

FIG. 8. (a) The angular transmittance of a *linear* Fabry-Pérot cavity coated on both sides with dielectric multilayer mirrors for TE-polarized fields. Parameters of the central Fabry-Pérot cavity: $d=5.775\ \mu$m, $\epsilon=2.46$. Parameters of the dielectric mirrors: $d_a=90$ nm, $d_b=80$ nm, $N=25$, $\epsilon_a=2.95$, $\epsilon_b=2.46$, $\epsilon_s=\epsilon_c=1$, θ is angle of incidence. The appearance of the Airy resonances within the stop gap is obvious [compare with Fig. 3(a)]. (b) Same geometry and type of curve as in (a), but for TM-polarized fields [compare with Fig. 3(b)].

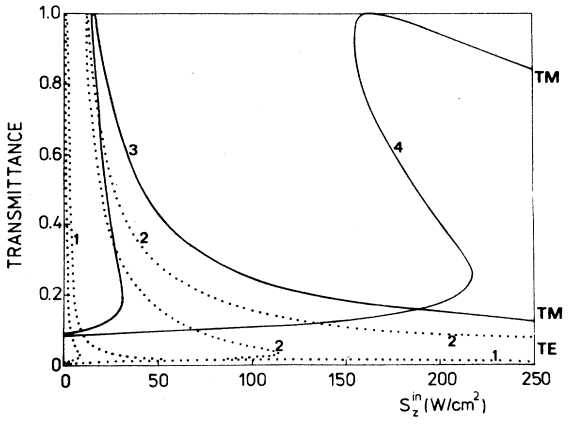

FIG. 9. The transmittance vs input flux $S_x^{\rm in}$—curves of *nonlinear* Fabry-Pérot cavities coated on both sides either with *linear* or *nonlinear* dielectric multilayer mirrors. The angle of incidence θ is fixed near an Airy resonance $\theta^{\rm res}$; both polarization types are considered. In the linear limit, all coated cavities coincide with the geometry of Figs. 8. Dotted curves; TE-polarization ; $\theta_{\rm TE}=53.4°$, $\theta_{\rm TE}^{\rm res}=52.9°$; solid curves, TM polarization; $\theta_{\rm TM}=53.8°$, $\theta_{\rm TM}^{\rm res}=53.1°$; curves 1 and 3, *nonlinear* coating ($n_{2b}=2\times10^{-3}$ m^2/W, $n_{2a}\equiv0$); curves 2 and 4, *linear* coating ($n_{2b}\equiv0$, $n_{2a}\equiv0$); *nonlinear* cavity, $n_2=2\times10^{-9}$ m^2/W; all other parameters as in Fig. 8.

ing reduces the switching power for both states of polarization considerably (see Fig. 9). When the nonlinearities in both the central cavilty and the endface coating have the same sign (both assumed positive in Fig. 9), the nonlinear detuning effects support each other thus lowering the switching power. This effect should be most pronounced with an Airy resonance in the vicinity of the appropriate stop band edge.

With regard to minimum switching power levels, TE-polarized fields are clearly preferred. On the other hand, the large transmittance differences in some input flux ranges indicate the occurrence of optical bistability with respect to the polarization angle to be highly likely.

V. SUMMARY

In conclusion, we have developed an algorithm that permits the calculation of the optical response of nonlinear multilayer systems irradiated by obliquely incident TM-polarized plane waves. We have demonstrated that various multilayer systems, illuminated on the appropriate slope of a linear resonance peak, can be driven towards a bistable behavior with respect to the input flux. For self-focusing nonlinearities, the higher-angle slopes of the linear resonance peaks become sensitive to backbending, i.e., optical bistability, and vice versa for defocusing nonlinearities. Low switching intensities require sharp linear resonance slopes.

Linear absorption effects will set fundamental limits in implementing switching operations. A comparison between the response behavior with respect to TE- and TM-polarized fields has revealed a clear advantage of TE-polarized fields regarding the switching intensities. This is mainly due to the sharper linear resonances of the systems under investigation in the TE case.

Our results suggest a bistable response behavior with respect to the polarization angle although the explicit demonstration requires the full inclusion of all three electric field components which will be left for a forthcoming publication.

Other challenges for further investigations are the consideration of both electronical as well as molecular reorientational nonlinearities which leads to anisotropic, nondiagonal dielectric tensors. Furthermore, the inclusion of nonlinear absorption and saturation effects will disclose the limits set for nonlinear materials in order to get bistable response curves. The demonstration of optical bistability with respect to both the angle of incidence and the wavelength of the input light implies merely a straightforward application of our algorithm and has not been added here.

[1]S. D. Smith, A. L. Walker, B. S. Wherrett, F. A. Tooley, J. G. H. Mathew, M. R. Taghizadeh, and T. Janossy, Appl. Opt. **25**, 1586 (1986).
[2]U. Trutschel, F. Lederer, and M. Golz, IEEE J. Quantum Electron. **QE-25**, 194 (1989).
[3]W. Chen and D. L. Mills, Phys. Rev. B **35**, 524 (1987).
[4]T. Peschel, P. Dannberg, U. Langbein, and F. Lederer, J. Opt. Soc. Am. B **5**, 29-35 (1988).
[5]W. Chen and D. L. Mills, Phys. Rev. B **38**, 12 814 (1988).
[6]W. Chen and D. L. Mills, Phys. Rev. B **36**, 6269 (1987).
[7]W. Chen and D. L. Mills, Phys. Rev. Lett. **58**, 160 (1987).
[8]D. L. Mills and S. E. Trullinger, Phys. Rev. B **36**, 947 (1987).
[9]U. Trutschel and F. Lederer, J. Opt. Soc. Am. B **5**, 2530 (1988).
[10]J. H. Marburger and F. S. Felber, Phys. Rev. A **17**, 335 (1978).
[11]H. G. Winful, J. H. Marburger, and E. Garmire, Appl. Phys. Lett. **35**, 380 (1979).
[12]S. Dutta Gupta and G. S. Agarwal, J. Opt. Soc. Am. B **4**, 691 (1987).
[13]O. Svelto, in *Progress in Optics XII,* edited by E. Wolf (North-Holland, Amsterdam, 1974), pp. 3–102.
[14]R. I. Joseph and D. N. Christodoulides, Opt. Lett. **12**, 826 (1987).